

1 Geographic variation in the genetic basis of resistance to leaf rust in locally
2 adapted ecotypes of the biofuel crop switchgrass (*Panicum virgatum*)
3

4 Acer VanWalleendael^{1,2}, Jason Bonnette³, Thomas E. Juenger³, Felix B. Fritsch⁴, Philip A. Fay⁵,
5 Robert B. Mitchell⁶, John Lloyd-Reilley⁷, Francis M. Rouquette Jr.⁸, Gary Bergstrom⁹, and
6 David Lowry^{1,2}
7

8 **Author Affiliations:**

9 ¹Department of Plant Biology, Michigan State University, East Lansing, MI, USA

10 ²Great Lakes Bioenergy Research Center, Michigan State University, East Lansing, MI, USA

11 ³Department of Integrative Biology, University of Texas at Austin, Austin, TX, USA

12 ⁴Division of Plant Sciences, University of Missouri, Columbia, MO, USA

13 ⁵USDA-ARS Grassland, Soil and Water Research Laboratory, Temple, Texas, USA

14 ⁶USDA-ARS Wheat, Sorghum, and Forage Research Unit, University of Nebraska, Lincoln, NE,
15 USA

16 ⁷USDA-NRCS, Kika de la Garza Plant Materials Center, Kingsville, TX, USA

17 ⁸Texas A&M AgriLife Research, Texas A&M AgriLife Research and Extension Center,
18 Overton, TX, USA

19 ⁹School of Integrative Plant Science, Cornell University, Ithaca, NY, USA
20
21
22
23
24
25
26
27
28
29
30
31

32 **Abstract**

33 Pathogens play an important role in the evolution of plant populations, but genetic
34 mechanisms underlying disease resistance may differ greatly between geographic areas as well
35 as over time. Local adaptation is thought to be an important step in plant evolution, and may be
36 impacted by differential pathogen pressures in concert with abiotic factors. This study uses
37 locally adapted ecotypes of the native perennial switchgrass (*Panicum virgatum*) to examine the
38 temporal and spatial variation in the genetic architecture of resistance to fungal pathogens,
39 namely switchgrass leaf rust (*Puccinia novopanici*). To identify loci underlying variation in
40 pathogen resistance in switchgrass, we scored rust damage across an outcrossed mapping
41 population at eight locations across the central United States from southern Texas to Michigan.
42 We followed rust progression at these sites for three years and mapped quantitative trait loci
43 (QTLs) using function-valued transformations of rust progression curves. Overall, we mapped 51
44 QTLs that varied in presence and strength over the three-year period. Two large-effect QTLs
45 were consistently associated with variation in rust progression in multiple sites and years, and are
46 therefore potentially the result of the same underlying resistance genes. Interestingly, these two
47 large-effect QTLs were almost exclusively detected in northern sites. This pattern could be
48 caused by geographic difference in genetic architecture. The distribution of rust strains or
49 variation in climatic conditions across the field sites could result in genotype-by-environment
50 interactions in efficacy of rust resistance loci. Beyond reducing rust damage by 34%, the
51 beneficial alleles at the two loci also increased biomass by 44%, suggesting a direct benefit by
52 pleiotropy or indirect benefit through genetic linkage. Our results suggest an important role for
53 fungal pathogens in the local adaptation of switchgrass and illustrate an influential geographic
54 component of the genetic architecture of plant disease resistance.

55

56 **Introduction**

57 Understanding the factors that determine how well a particular population is adapted to
58 its environment is a major goal of evolutionary biology. Plant populations often exhibit local
59 adaptation, in which populations are more successful in their local environments than foreign
60 genotypes in that environment (Leimu & Fisher 2008; Kawecki & Ebert 2004). Traditional
61 studies of local adaptation have focused on the abiotic factors that contribute to differential
62 population success (e.g. Clausen et al. 1940). Recent advances in molecular biology have

63 allowed researchers to directly link abiotic stresses to genetic differences between populations,
64 showing variation in the genetic basis of local adaptation (McKay et al. 2003; Lowry & Willis
65 2010; Fournier-Level et al. 2011; Price et al. 2018; He et al. 2018). However, biotic interactions
66 have been less-studied in this context, but may be essential for explaining variation in local
67 adaptation (Macel et al. 2007; Grøndahl & Ehlers 2008; Crémieux et al. 2008). Pathogens can
68 impose strong disruptive selection on plant populations when they are constrained in the areas
69 they infect, and therefore shape local adaptation (Giraud et al. 2017; Mursinoff & Tack 2017).
70 Therefore, a full understanding of plant adaptation requires characterization of the genetic basis
71 of local adaptation to pathogens in conjunction with the abiotic environment.

72 Molecular coevolution between microbe and host has been documented throughout the
73 tree of life (Hooper & Gordon 2001; Gagneux et al. 2006; Alfano & Collmer 2004; Dodds et al.
74 2006) and is an important tool to understand large-scale evolution (Moran et al. 2008;
75 Woolhouse et al. 2002). The most basic genetic mechanism underlying this dynamic is a gene-
76 for-gene interaction, whereby infection success is determined by variation at a single locus in
77 both the pathogen and host (Agrios 1997; Kniskern & Rausher 2006). In the host, resistance (R)
78 genes usually code for proteins that recognize either the direct product of a single pathogen gene
79 or some downstream protein in its signaling pathway (Jones & Dangl 2006). Pathogen genes that
80 have a corresponding R-gene in their host are termed ‘avirulence’ genes because their presence
81 means that plant resistance will be effective. Plant R-gene products trigger a cascade of changes
82 in response to the avirulence gene that may result in the hypersensitive response and systemic
83 acquired resistance (Kniskern & Rausher 2006). The hypersensitive response (HR) is a local
84 upregulation of various protective mechanisms, including production of reactive oxygen species
85 (ROS) and free radicals that may kill a pathogen, but typically at the cost of cell death and
86 possible loss of fitness and growth (Tian et al. 2003; Jones & Dangl 2006). Systemic acquired
87 resistance (SAR) is more akin to an innate immune response in vertebrates, whereby pathogen
88 recognition molecules are increased in expression throughout the plant, improving resistance to
89 later infections (Jones & Dangl 2006). SAR also shows a fitness cost, but has been demonstrated
90 to maintain fitness under disease pressure (Traw et al. 2007).

91 The gene-for-gene coevolutionary model is appealingly simple and can sometimes
92 explain the pattern of race-specific resistance in many plant species (e.g. van Leur et al. 1989).
93 However, quantitative resistance may also evolve, whereby resistance is governed by allelic

94 composition at several to many loci (Geiger & Heun 1989; Agrios 1997; Young 1996). These
95 mechanisms are typically more complex, involving polygenic adaptations for morphological or
96 phenological changes, production of antimicrobial compounds, and modification of effector
97 targets (Niks et al. 2015). Studies have found several examples of both gene-for gene resistance
98 (Kniskern & Rausher 2006; Bourras et al. 2016), and quantitative resistance (Quesada et al.
99 2010), but little consensus on the factors that determine which will evolve in a particular system.
100 Rather, it appears that the expression of host resistance as well as parasite virulence are
101 environmentally-dependent traits, not stable phenotypes as has been traditionally assumed
102 (Penczykowski et al. 2016). Since resistance mechanisms are generally investigated under either
103 stable laboratory conditions or at a single field site, it is challenging to breed for durable
104 resistance, resistance that prevents disease in many locations and for more than a few years
105 (Mundt 2014). Addressing the environmental variation in the genetic architecture of plant
106 disease resistance requires an experiment replicated over both time and space.

107 The prairie grass switchgrass (*Panicum virgatum*) and its obligate fungal pathogen,
108 switchgrass leaf rust (*Puccinia novopanici*), are an ideal system to study how loci contributing to
109 pathogen resistance vary across space. *Panicum virgatum* L. is a long-lived, polyploid, C4,
110 perennial grass native to North America east of the Rocky Mountains from northern Mexico to
111 southern Canada (Gleason and Cronquist 1991). It is a common prairie and pasture grass and is
112 grown as both a forage crop and as a bioenergy feedstock (Casler 2012; Parrish et al. 2012), and
113 has become an important study system for ecological specialization. *P. virgatum* is split into two
114 locally adapted ecotypes, upland and lowland (Morris et al. 2011; Lowry et al. 2014; Milano et
115 al. 2016). The upland ecotype is more common in northern North America, and exhibits small
116 stature (up to 190 cm) and low pathogen resistance (Casler 2012; Uppalapati et al. 2013; Milano
117 et al. 2016; Lovell et al. 2016). In contrast, the more southerly lowland ecotype is large (up to
118 285 cm) and is more resistant to fungal pathogens (Casler 2012; Uppalapati et al. 2013; Milano
119 et al. 2016; Lovell et al. 2016). While the lowland ecotype produces more biomass, it also has
120 lower freezing tolerance (Lee et al. 2014; Peixoto & Sage 2016), possibly explaining the rarity of
121 lowland ecotypes in more northern climates.

122 Since *P. virgatum* ecotypes differ in their susceptibility to rust infection, this host-
123 pathogen system is useful for testing the role of local variation in the evolution of resistance.
124 Switchgrass is infected with at least five species of rust (*Puccinia spp.*; Demers et al. 2017), but

125 *Puccinia novopanici* is thought to be dominant in the central US (Gary Bergstrom, *pers. obs.*). *P.*
126 *novopanici* is a basidiomycete fungi that infects only living leaf tissue of *P. virgatum*. As such,
127 these fungi are thought to be extirpated from northern populations every winter. In closely-
128 related and well-studied wheat rust (*P. triticana*), wind-borne spores blow from warm refugia in
129 southern Texas across the Great Plains every summer in what is known as the “Puccinia
130 pathway” (Eversmeyer & Kramer 2000). While this has not been directly examined for
131 switchgrass rust, it is the dominant explanation for epidemiological patterns, and fits with our
132 observations. Rust infection is virtually inevitable in switchgrass stands in North America by the
133 late summer, though damage is less severe in varieties from the lowland ecotype.

134 Over the range of switchgrass in North America, plant-pathogen interactions occur in a
135 wide range of abiotic conditions. The environmental dependence of resistance can have
136 important consequences for disease prediction and breeding for durable resistance (McDonald &
137 Linde 2002; Michelmore et al. 2013). In *Nicotiana*, for instance, elevated temperature inhibits
138 plant defense responses, prompting a need for development of heat-resistant R-genes (Zhu et al.
139 2010). The reasons for altered pathogenicity in different climates can be due to failure of plant
140 defenses as a result of multiple causes, including stress (Zhu et al. 2010), promotion of beneficial
141 pathogen conditions (Doke 1983), and variation in pathogen ecology (Weller et al. 2002). While
142 there have been few studies of the environmental niche of switchgrass rusts, closely related
143 wheat rusts can offer some clues. In wheat stripe rust (*P. striiformis*), resistance genes are
144 temperature-dependent (Fu et al. 2009). Further, it is well-established that variation in humidity
145 can greatly impact the infection by foliar fungal pathogens (Magarey et al. 2005), and may
146 therefore play a role in plant resistance. Thus, over the geographic range of the switchgrass-rust
147 interactions, variation in the abiotic environment may play an important role in influencing both
148 plant defenses and pathogen virulence.

149 The primary goal of our study was to characterize the genetic architecture of switchgrass
150 resistance to rust pathogens to better understand the causes of pathogen-mediated local
151 adaptation. To overcome past limitations due to environmental and temporal variation in host-
152 pathogen relationships, we measured fungal resistance over three years at a continental scale. We
153 planted clonally replicated quantitative trait locus (QTL) mapping populations at eight sites
154 across more than 7000 km of latitude to map QTLs for rust resistance. We first tested whether
155 rust resistance is controlled by large-effect loci corresponding to specific pathogens in a gene-

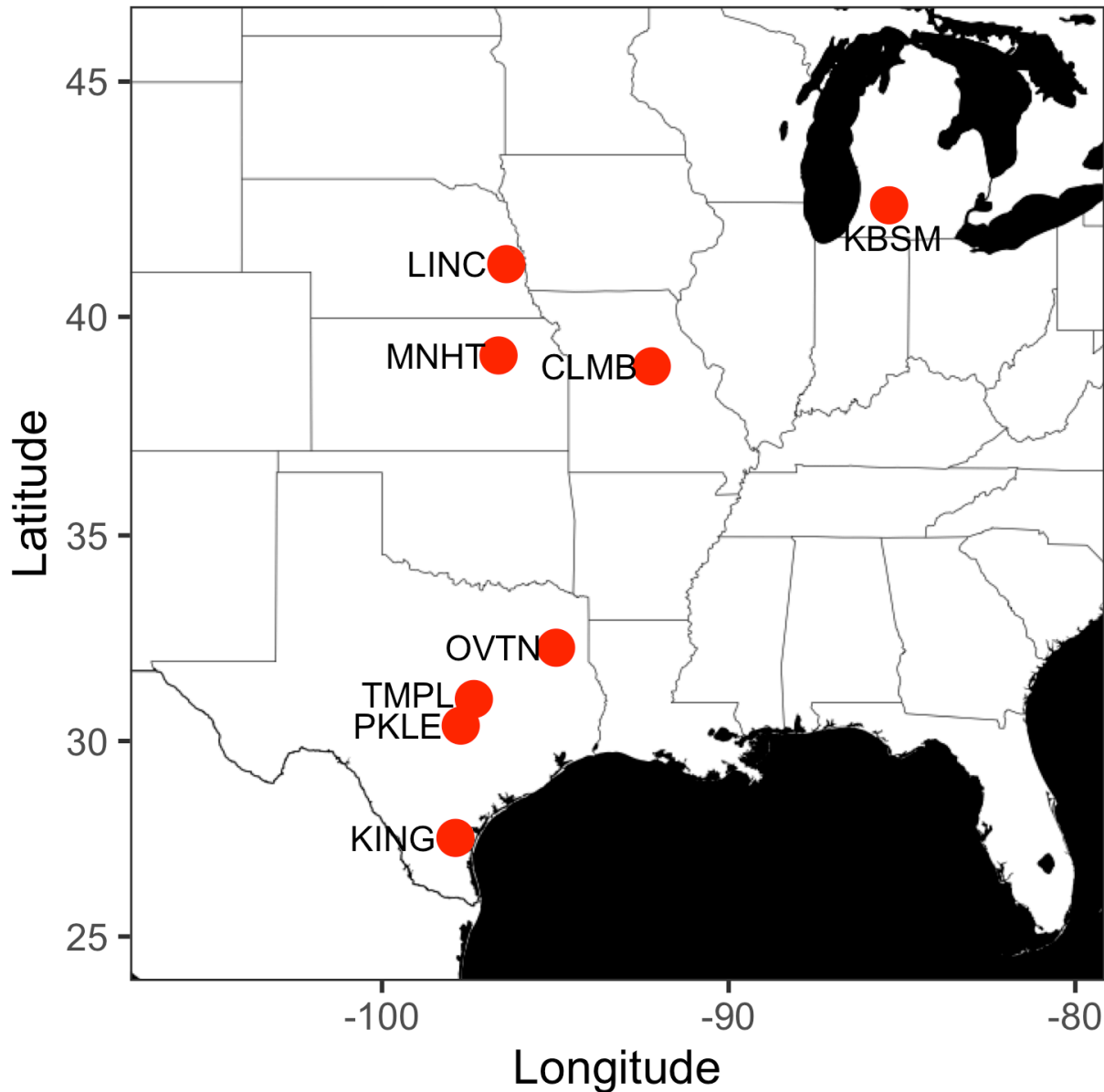
156 for-gene model or by small-effect loci in a polygenic resistance model. The geographic patterns
157 of QTL presence and strength allowed us to fully summarize the spatial distribution of pathogen
158 resistance. Therefore we were able to test the degree to which resistance exhibits a genotype-by-
159 environment interaction, or is homogeneously expressed. In addition, we assessed the
160 quantitative impact of those QTLs on resistance and other morphological and fitness traits to
161 determine the evolutionary impacts of pathogen resistance. We hypothesized that resistance
162 alleles would have evolved in lowland ecotypes and would be correlated with morphological
163 differences between ecotypes, such as biomass and tiller count.

164

165 **Methods**

166 *Development of mapping populations*

167 To identify loci controlling variation in rust progression, we used a previously developed
168 a four-way phase-known (pseudo-testcross) population (for full cross details, see Milano et al.
169 2016). We clonally divided the outbred populations by manually splitting rhizomes at the
170 Brackenridge Field Laboratory in Austin, TX. In May-July of 2015, the F_0 , F_1 , and F_2 clones
171 were potted, moved by truck, and transplanted at eight sites (Figure 1) in Kingsville, TX; Austin,
172 TX; Temple, TX; Overton, TX; Columbia, MO; Manhattan, KS; Mead, NE; and Hickory
173 Corners, MI. We assigned plants randomly to a honeycomb design, with 1.56 m between each
174 plant. To reduce edge effects, we planted a border of lowland plants around the plot that were not
175 measured experimentally. We watered plants by hand in 2015 to facilitate establishment. To
176 develop a linkage map for QTL mapping we genotyped 431 second-generation genotypes by
177 whole genome resequencing (for full details, see Lowry et al. 2019).



178
179 **Figure 1:** Locations of experimental sites in central North America. KING: Kingsville, TX;
180 PKLE: Austin, TX; TMPL: Temple, TX; OVTN: Overton, TX; CLMB: Columbia, MO; MNHT:
181 Manhattan, KS; LINC: Mead, NE; KBSM: Hickory Corners, MI.

182
183 *Phenotyping*

184 At each site we scored the presence of leaf rust in 2016, 2017, and 2018. We used a
185 method developed for rust on wheat (*Triticum aestivum*; McNeal et al. 1971; Roelfs et al. 1992),
186 which translates well to switchgrass and has been used in previous studies (Uppalapati et al.

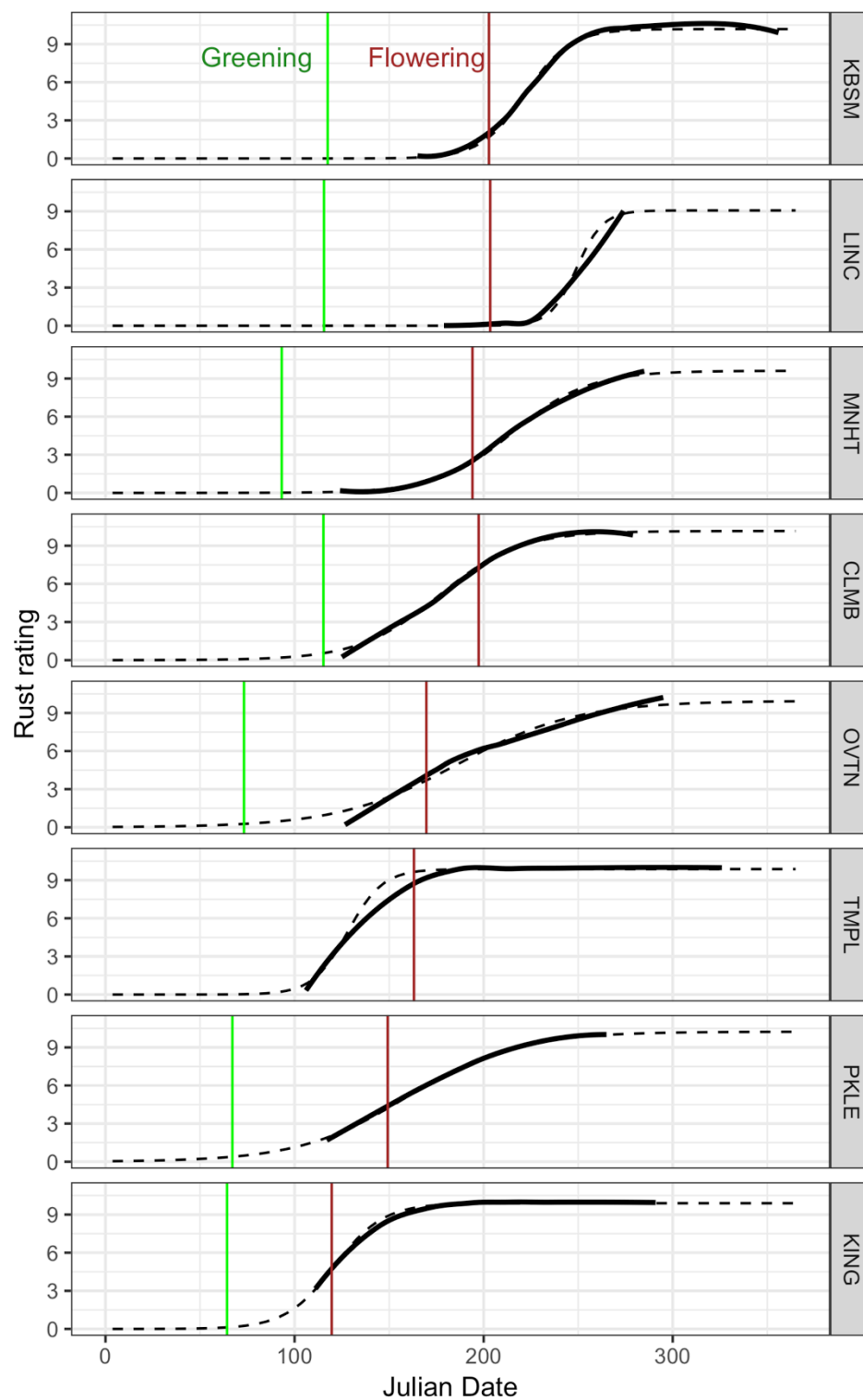
187 2013). At each site, we scored rust on a 0-10 scale based on the total proportion of the canopy
188 covered in rust spores, a score which we have defined as ‘rust damage’ for this study (Figure 2).
189



190
191 **Figure 2:** A. Heavily infected single leaf. B. Lightly infected small plant.
192

193 In conjunction, we used a simple resistance definition as $1 - \text{rust damage}$ (Simms & Triplett
194 1994). Other fungal pathogens such as anthracnose and *Bipolaris* were present in plots, but were
195 generally less common than rust and were not reflected in our ratings.

196 The effort extended to phenotyping rust damage varied among sites and years due to
197 logistical challenges. However, for the most part, sampling began three weeks after green-up (the
198 point at which ~50% of plants had emerged from the soil) and continued weekly until damage
199 stopped increasing (Figure 3). Over three years, this resulted in over 149,000 rust ratings, which
200 were used for the QTL analyses. In addition, we measured other morphological and
201 physiological traits at all sites, including the number of tillers, weekly plant height, date of first
202 flowering, and end-of-season aboveground biomass (see Milano et al. 2016 and Lowry et al.
203 2019 *in review* for details of this phenotyping effort).



204

205 **Figure 3:** Rust progression curves in 2016. Black lines show smoothed mean rust values for

206 sampled dates, black dotted lines show fitted logistic curves to sampled data. Green and brown

207 vertical lines show green-up date and date of first flowering, respectively. (2017 & 2018 in
208 Supp.)

209

210 *Rust abundance and composition*

211 Visual pathogen scoring regimes are well known to be subject to statistical artifacts
212 (Lesaffre et al. 2012) and our data were no exception. Pathogen scores followed a tail-inflated
213 (“U”-shaped) distribution. Therefore, we used nonparametric Wilcoxon signed-rank and
214 Kruskal-Wallis tests using the functions *wilcox.test* and *kruskal.test* in the *stats* package of R to
215 test the differences in damage between lineages, years, and sites (R core team 2018). To test for
216 cytoplasmic effects on rust prevalence, we compared rust scores between F₂ individuals with
217 maternal cytoplasm from upland and lowland F₁S, also with the aforementioned nonparametric
218 tests.

219

220 *Genomic architecture*

221 We first mapped QTLs using traditional QTL mapping on pathogen ratings for each
222 individual time point. Raw pathogen ratings were processed in R (v3.4; R core team 2018) using
223 both packages *qtl* and *funqtl* (Broman et al. 2003; Kwak et al. 2016). To examine QTL effects
224 over time, we scanned for QTLs using Haley-Knott regression for each site by year combination,
225 with each time point as a separate trait using the functions *scanone* in *qtl* and *geteffects* in *funqtl*
226 (Broman et al. 2003; Kwak et al. 2016).

227 We additionally examined QTLs controlling the overall progression of rust by modeling
228 damage as a function-valued trait (Kwak et al. 2014; 2016). For each individual, we fit a curve to
229 rust damage ratings using the R package *funqtl* (Kwak et al. 2016). This method has the
230 advantage of decreasing bias introduced by differences among raters at different sites by using
231 the parameters of an damage curve as traits, rather than the absolute rating values. In addition, it
232 overcomes several statistical challenges of QTL mapping of time-valued traits by replacing trait
233 data with a smoothed approximation, then applying functional principal component analysis
234 (FPCA) as a dimension-reduction technique (Kwak et al. 2016). QTLs are then mapped for a
235 small number of principal components (PCs; Kwak et al. 2016). These PCs represent the shape
236 of the pathogen damage curve of rust, and therefore include both the timing and rate of infection
237 spread. Previous studies have used area under disease progress curve (AUDPC) measurements to

238 quantify resistance (Jeger & Viljanen-Rollinson 2001). AUDPC is robust and useful, but may
239 show bias when infection timing differs among sites (Jeger & Viljanen-Rollinson 2001). FPCA
240 generally shows the same results as AUDPC, but is less impacted by phenology differences. We
241 used the first four PCs to map QTLs, and combined their effects by taking the mean LOD
242 (logarithm of the odds) score, the SLOD score, at each genomic position (Kwak et al. 2016).
243 Then we conducted 1000 permutations to calculate a penalty for the SLOD score that reduces the
244 rate of inclusion of extra loci to 5% (Broman & Sen 2009). We examined geographic and
245 temporal variation by mapping QTLs separately for each site and year, but we also generated a
246 combined test that summarizes variation in this experiment. For this test, we summed SLOD
247 scores across multiple sites and years, and concatenated permutations to generate a critical
248 SLOD cutoff. We produced all plots using *funqtl* and *ggplot2* (Kwak et al. 2016; Wickham &
249 Wickham 2007).

250 Finally, we estimated the allele-specific effects of the significant QTLs we discovered in
251 our study. In the four-way cross design, second-generation offspring can express four possible
252 allele combinations, L1_L2, U2_L1, U1_L2, or U1_U2. These represent alleles from each of the
253 four parents (lowland AP13: L1; lowland WBC: L2; upland DAC: U1; and upland VS16: U2).
254 For each locus, we compared the pathogen scores for the individuals with the “resistant” QTL
255 alleles to those with the “susceptible” alleles. We additionally made this comparison for
256 morphological traits including biomass, flowering time, tiller count, and green-up date. We
257 tested for difference in means using nonparametric Wilcoxon signed-rank tests for pathogen
258 ratings, and a two-sample *t*-test for all morphological traits.

259

260 **Results**

261

262 *Rust abundance and composition*

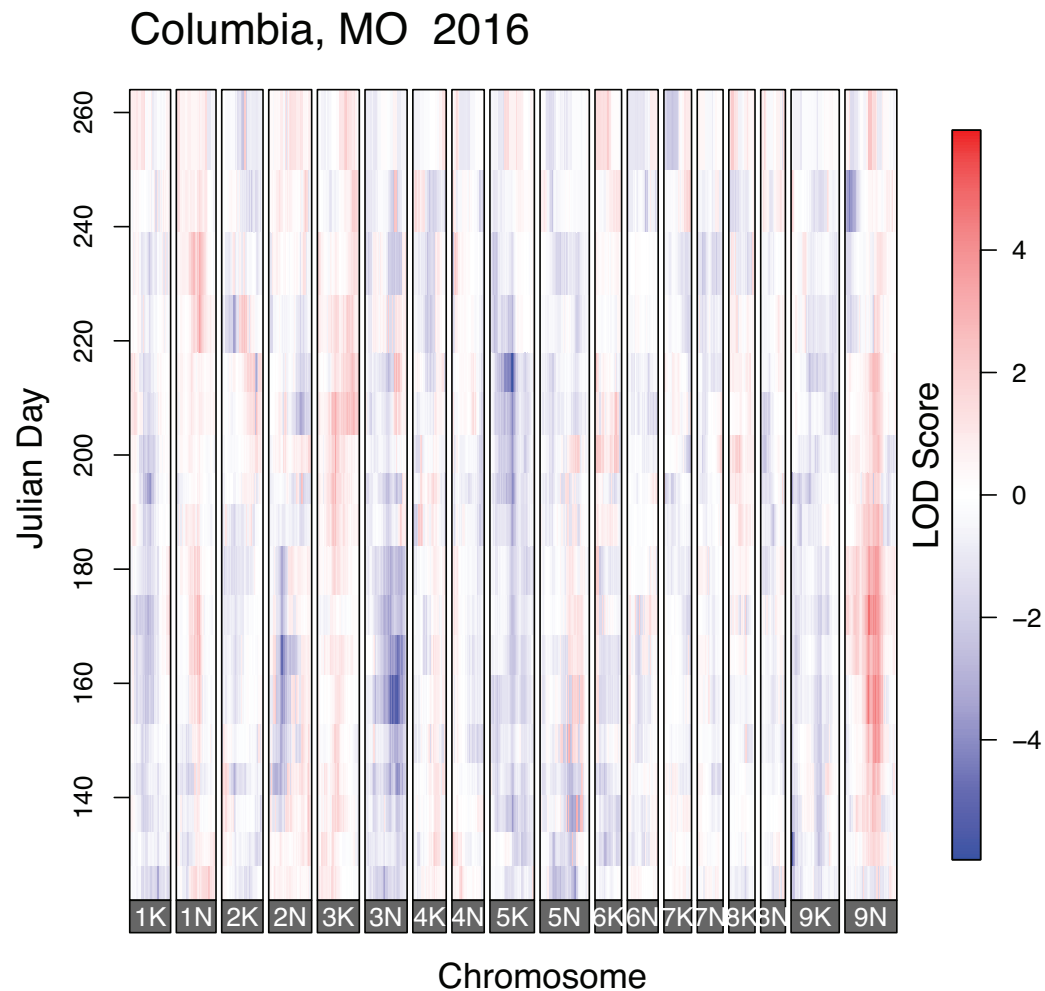
263 Though infection timing varied, rust was present at all sites throughout the study period
264 (Figure 3). The largest genetic source of variation was between upland and lowland F0
265 (grandparental) plants, with upland plants experiencing 39.15% more rust damage ($W = 1.15e7$,
266 $p < 0.0001$). Rust damage differed between generations in the cross ($\chi^2 = 656.98$, $p < 0.0001$),
267 with F₀ plants showing the least amount of rust, and F₁ plants the greatest (Figure S1). Rust
268 damage was negatively correlated with green-up date, biomass, flowering time, height, and tiller

269 count (Figure S2). Field sites differed significantly in mean rust damage across years ($\chi^2 =$
270 1.99e5, $p < 0.0001$), though this was confounded by differing sampling periods across sites.
271 Mean rust damage declined in almost every site each year (Figure S3), decreasing by 19.75% in
272 2017 and 30.74% in 2018. This change correlates with biomass increases of 85.64% in 2017 and
273 46.89% in 2018. Our cross design allowed us to test the phenotypic effect of maternal cytoplasm,
274 the difference between second-generation plants with an upland dam and those with a lowland
275 dam. We compared rust scores between second-generation individuals with maternal cytoplasm
276 from upland and lowland F_1 s. There was a cytoplasmic effect ($W = 1.72e9$, $P = 0.0059$), but rust
277 scores were only 1.33% higher in plants with lowland cytoplasm (Figure S1).

278

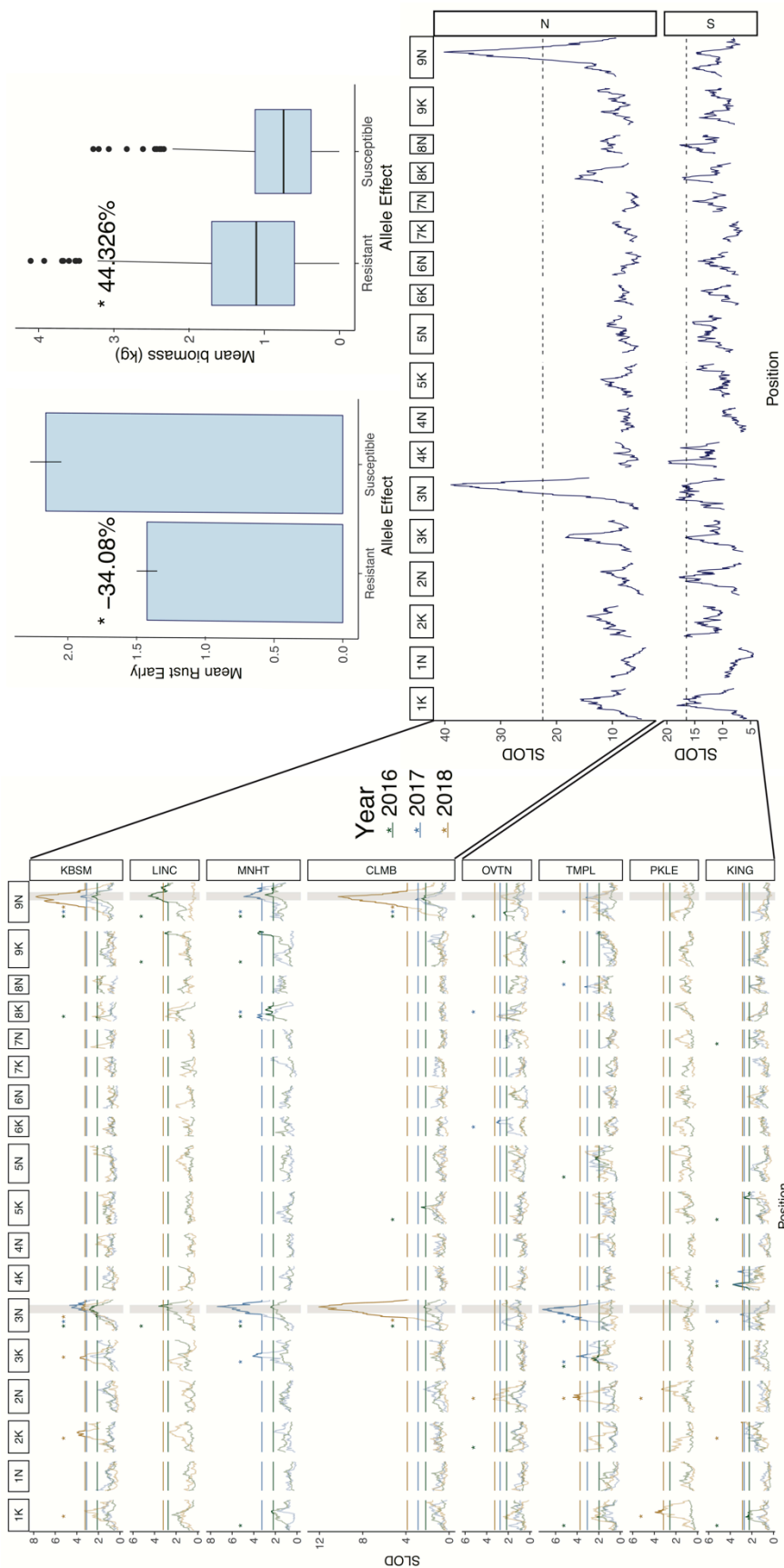
279 *Genomic architecture*

280 Since we collected data on pathogens over several weeks at all sites, we were able to
281 examine how the genomic architecture of resistance changed over a single season at each site by
282 scanning for QTLs as if each time point were a distinct phenotype. We found extensive variation
283 between sites, but some patterns were shared across several sites. We identified QTLs for
284 resistance at multiple sites on chromosomes 9N and 3N, though they differed in effect direction
285 (Milano et al. 2016). That is, the allele from a lowland grandparent decreased rust damage on
286 chromosome 9N, but increased damage on chromosome 3N. These QTLs had significant effects
287 for ~40-50 days, with the 9N QTL becoming detectable about one week after the 3N QTL
288 (Figure 4 and Supp.). Overall patterns were similar across years, although the collection of fewer
289 time points in 2017 resulted in lower-resolution data.



290
291 **Figure 4:** Time-series QTL effects for Columbia, MO in 2016 (remaining sites & years in
292 Supp.). Blue indicates that the lowland allele decreases rust, red indicates that the upland allele
293 decreases rust. Color intensity is proportional to LOD score, or the strength of the QTL.

294
295 We mapped 51 total QTLs using function-valued traits (Figure 5). Overall, we found the
296 highest number of QTLs at the most northern site (KBSM), though there was not a clear
297 geographic pattern in QTL number. Additionally, there was variation between years, with the
298 greatest number of QTLs in 2016 (24 QTLs), and fewer in 2017 and 2018 (15 and 12,
299 respectively). We found the same large-effect QTLs using function-valued traits to map overall
300 QTLs (Figure 5). Across several sites and all years, QTLs on chromosomes 3N and 9N had the
301 highest LOD scores (Figure 5), indicating close associations between loci and pathogen
302 resistance, and each explained ~14% of the variation in rust damage.



303

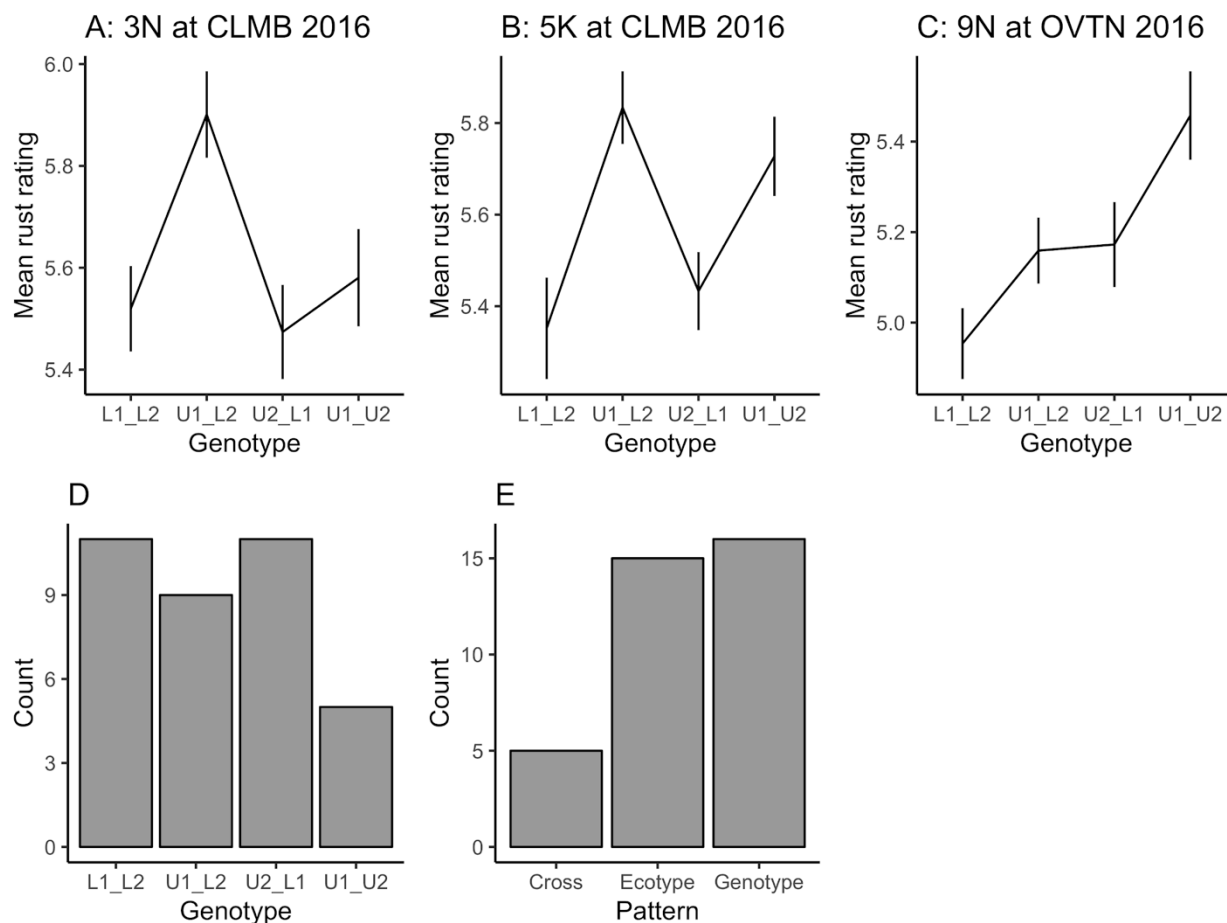
Figure 5: QTLs for all sites and years. SLOD shows the mean log-odds score for function-valued traits, or the strength of the QTL. Horizontal lines show significance thresholds for each test, peaks above the threshold are shown as solid lines, and peaks below as faded lines. Vertical gray bars highlight large-effect QTLs on chromosomes 3N and 9N. Asterisks show chromosomes that had at least one significant QTL and are colored by year. The combined SLOD plot shows SLOD scores summed over Northern and Southern sites. The bar charts show the phenotypic effect of the large-effect QTLs on rust infection and biomass.

304 Given their strength and consistency across sites and years, we considered these the most
305 important QTLs. These large-effect QTLs differed greatly between northern sites and southern
306 sites. LOD scores were significant at the large-effect sites in northern sites 17 times over the
307 three years, but only four times in southern sites.

308

309 *Allelic effects*

310 We calculated allele-specific effects for each QTL in our dataset to quantify the direction
311 and strength of each QTL. To understand the alleles underlying each QTL, we categorized them
312 into either “Ecotype-specific” or “Genotype-specific” based on the resistance of each
313 grandparental allele (Figure 6bc; Milano et al. 2016). For instance, if both upland alleles showed
314 higher rust damage, and both lowland alleles low rust damage, this QTL would be considered
315 ecotype-specific. If only one of the grandparental genotypes was resistant or susceptible, we
316 scored that as genotype-specific. We added an additional category, “Cross-specific,” for effects
317 that were shown in particular upland/lowland combinations (Figure 6a). A majority of loci
318 showed genotype-specific effects (31 out of 51). Relatively fewer showed ecotype-specific
319 effects (16 out of 51) and cross-specific effects were rarest (4 out of 51). In addition, we counted
320 the number of resistance QTLs for each grandparental allele (Figure 6d). Many loci were in the
321 same direction as the parental divergence, with both lowland alleles causing a reduction in rust
322 prevalence (23 out of 51), but the same number showed the lowest rust with an upland/lowland
323 allele combination. A few (5 out of 51) showed opposite pattern, with the least rust with both
324 upland alleles (Figure 6e).



325

326

327

328 **Figure 6:** Pattern of allele-specific effects for significant QTLs. A-C: Examples of three possible

329 patterns of allele-specific effects, cross-specific, genotype-specific, and ecotype-specific. D:

330 Frequency of all QTLs showing the lowest rust score. E: Frequency of each possible pattern of

331 allele-specific effects for all QTLs.

332

333 We then calculated the combined effects of the two large-effect QTLs we identified by
334 examining only individuals containing either resistant or susceptible combinations of alleles at
335 these loci. For instance, the allele from the upland VS16 grandparent was most resistant at the
336 9N locus, but the allele from the lowland WBC3 grandparent was most resistant at the 3N, so the
337 individuals with both of these alleles had the “resistant” combination of alleles. We also chose
338 the individuals with alleles that increased rust, that had the “susceptible” combination of alleles.
339 By comparing these individuals, we estimated the phenotypic impacts of our large-effect QTLs.

340 The effects of QTLs were most apparent early in the season, when the “resistant” combination
 341 resulted in 34.08% lower rust scores ($W = 56156$, $P = 0.0003$). Later in the summer, the
 342 difference between resistant and susceptible decreased to 6.22%, but variation also decreased (W
 343 $= 41666$, $P < 0.0001$). We repeated this comparison for several other morphological variables.
 344 The resistance alleles increased biomass by 44.3% ($t = 5.44$, $P < 0.0001$, Figure 5), tiller count
 345 by 7.59% ($t = 2.58$, $P = 0.010$), and height by 5.52% ($t = 6.12$, $P < 0.0001$), and contributed to a
 346 2.07% later flowering time ($t = 2.04$, $P = 0.041$; Table 1).

347
 348 **Table 1:** Allele-specific effects for the combination of the 3N and 9N QTLs for rust resistance.
 349 “Resistant” represents the mean values for individuals with alleles that decrease rust,
 350 “Susceptible” represents mean values for individuals with alleles that do not confer resistance.
 351 Bold values are significant at $\alpha = 0.05$.

352

	Susceptible	Resistant	Δ	Statistic	P
Rust score	2.161	1.425	34.08%	W = 56156	0.0002
Biomass (g)	480	607	26.48%	t = 5.444	<0.0001
Flowering time (Julian Day)	177	180.6	2.07%	t = 2.041	0.0415
Tiller Count	130.9	140.9	7.59%	t = 2.581	0.0100
Height (cm)	154.4	163	5.52%	t = 6.116	<0.0001

353

354 Discussion

355 Our results show that there is a marked difference between the genetic architecture of rust
 356 resistance between populations planted in northern and southern regions. In the north, resistance
 357 appears qualitative, and driven by two large-effect loci that explain ~14% of variation in rust
 358 damage, and clearly influence plant morphological traits. These QTLs were largely stable across
 359 all three years of the study, indicating that they confer durable resistance. In the south, resistance
 360 is more quantitative, driven by many small-effect loci that vary year-to-year.

361 We found support for a gene-for-gene model in northern populations, but southern
 362 populations were representative of polygenic resistance. This geographic difference leads us to
 363 conclude that there is a strong genotype-by-environment interaction for rust resistance in

364 switchgrass. Our hypothesis that the majority of resistance QTLs evolved in the lowland
365 ecotypes was supported, but at many loci, an upland-lowland allele combination produced the
366 greatest rust resistance. We also found support for the hypothesis that resistance alleles are
367 correlated with morphological differences, indicating that the two large-effect loci we mapped in
368 the north may have contributed to ecotypic differentiation between upland and lowland *P.*
369 *virgatum*. Overall, our results suggest an important role for two large-effect loci in northern
370 populations, but primarily minor effect loci underlying variation in resistance at southern field
371 sites.

372

373 *Genomic architecture*

374 Locally adapted northern upland and southern lowland ecotypes of *P. virgatum* are
375 divergent for many traits (Casler et al. 2004, 2007; Lowry et al. 2014; Milano et al. 2016; Lowry
376 et al. 2018 *in review*), including cold tolerance, biomass, and leaf architecture (Casler 2012
377 p.30). Ecotypic differences in fungal pathogen resistance have been well documented for *P.*
378 *virgatum* and will play a key role in the success of switchgrass as a forage and biofuel crop
379 (Cornelius & Johnston 1941; Uppalapati et al. 2012; Sykes et al. 2016). Both of the large-effect
380 resistance QTLs colocalize with previously-identified large-effect QTLs for biomass, height, and
381 tiller number using the same mapping populations (Lowry et al. 2019 *in review*).

382 The most striking pattern in QTLs over time and space was between northern and
383 southern sites. In the north, the two large-effect QTLs are consistently present over time and
384 across four sites. This pattern would be expected for qualitative gene-for-gene resistance, in
385 which the two QTL peaks are caused by resistance genes on chromosomes 3N and 9N. However,
386 in the south, there are many more small-effect QTLs. This pattern is more indicative of
387 quantitative resistance (Corwin & Kliebenstein 2017). It is possible that the large-effect QTLs in
388 the northern sites obscured several small-effect QTLs that would have otherwise been above the
389 critical LOD score, a phenomenon known as the Beavis effect (Beavis 1998; Xu 2003). The
390 Beavis effect obscures small-effect QTLs and causes effect size overestimation of detected QTLs
391 (Xu 2003). However, this bias is greatly decreased in sample sizes near to 500, so we expect that
392 the impact on our study was minimal.

393 Typically, resistance to a particular pathogen is either quantitative or qualitative, but this
394 pattern is not generally thought of as being geographically dependent. Studies in wheat have

395 found that rust resistance can be geographically constrained because resistance is typically strain-
396 specific (Kolmer 2005). Since rust populations in the central US are dominated by a single
397 species, *P. novopanicum* (Gary Bergstrom *pers. obs.*), resistance differences are inconsistent with
398 species differences. Rather, we expect that north-south resistance differences may either be
399 driven by differences in rust strain diversity or a GxE interaction on the resistance loci. Broadly,
400 we expect higher strain diversity in the south, since this pattern has been documented for wheat
401 rust in Asia (Ali et al. 2014) and anther smut in *Silene* (Bueker et al. 2016). Southern populations
402 may have responded to higher stain diversity with more resistance loci. Alternatively, resistance
403 may be environment-dependent, as a study found for temperature-dependent resistance to wheat
404 stripe rust (*Puccinia striiformis f. sp. tritici*; Fu et al. 2009). In wheat stripe rust and other
405 systems, immunity-related proteins often exhibit temperature-dependent activity (Franklin &
406 Wigge 2014), suggesting a potential mechanism for GxE in disease resistance. Further work in
407 this system should focus on quantifying the population genetics of *P. novopanicum* to better
408 understand whether resistance is strain-specific.

409 Previous efforts to map QTLs for rust resistance in switchgrass yielded limited results.
410 Milano et al. (2016) mapped one QTL on chromosome 8K for a rust prevalence in a population
411 planted in Austin, Texas. We found small-effect QTLs on this chromosome at three field sites,
412 but these loci were not consistently detected across years. The differences in QTLs may be due
413 to temporal differences, but are more likely traceable to inconsistency in phenotyping by
414 different field technicians. The previous study scored only five tillers per plant and used
415 principal-component transformation of a 1-4 rating scale (Milano et al. 2016). Our study
416 improved upon this method as we evaluated rust damage on a whole-plant basis and mapped
417 QTLs to function-valued transformations of rust progression, allowing for less bias due to tiller
418 selection and evaluation of the full rust progression curve.

419

420 *Allelic effects*

421 For the two large-effect QTLs, one showed higher resistance with the upland allele, and
422 the other with the lowland allele (Figure 5). This is surprising given that the lowland ecotypes
423 typically display the highest rust resistance (Uppalapati et al. 2013), so one might expect that all
424 resistance alleles would come from lowland plants. The presence of upland resistance alleles

425 may provide further evidence that pathogens differ between the north and south, since upland
426 plants are much more common in the north.

427 Previous studies of switchgrass found many fixed differences between ecotypes (Milano
428 et al. 2016), and considerable variability in effects of loci across geographic locations (Lowry et
429 al. 2019, *in press*). Our pathogen resistance results were similar, although a surprising number of
430 loci had genotype-specific effects. This may indicate divergent selection within ecotypes, and
431 that mechanisms for pathogen resistance differ between populations of the same ecotype, as
432 would be expected if pathogen strain differences are substantial. A similar pattern was found in
433 melon (*Cucumis melo*), in which resistance QTLs vary between cultivars due to differences in
434 *Fusarium* strains (Percepied et al. 2005). Since the lowland grandparental genotypes were much
435 more rust-resistant than the upland, it was surprising that the most rust-resistant plants expressed
436 resulted from a combination of an upland and a lowland alleles across QTLs.

437 The two large-effect QTLs decreased rust substantially throughout the season, though the
438 effect decreased over time. Leaf rust may show differing mechanisms of seedling and adult plant
439 resistance, so this pattern is not unexpected (German & Kolmer 1992). Similarly, resistance
440 alleles were associated with higher biomass and other overall morphological traits. This result
441 runs contrary to the expectation of a growth-defense tradeoff, whereby resistant genotypes
442 should be slower-growing due to limited resources (Herms & Mattson 1992). However, there
443 may be many reasons why a negative correlation between growth and defense does not occur
444 (Kliebenstein 2016; Hahn & Maron 2016). In switchgrass, we find that resistance QTLs
445 colocalize with biomass and tiller count QTLs (Lowry et al. 2019 *in review*), suggesting either
446 close linkage or a pleiotropic effect. Importantly for the emerging perennial bioenergy industry,
447 the correlation between resistance and biomass indicates that breeding switchgrass will be able to
448 combine positive traits without major trade-offs in biomass across most environmental
449 conditions. However, both biomass and resistance may instead trade off with freezing tolerance,
450 which is an important survival trait for switchgrass in high latitudes (Lowry et al. 2019 *in*
451 *review*). The major barrier to high-yield lowland traits in northern climates is winter
452 temperatures, so identifying the molecular basis of upland freezing tolerance in switchgrass is an
453 important goal. If freezing tolerance is not linked to rust resistance, there is great potential for
454 improvement of switchgrass for biofuel, especially in northern marginal areas.

455

456 **Conclusion**

457 Our results show the temporal and geographic variation in the genetic architecture of rust
458 resistance in locally adapted switchgrass, including two large-effect loci that explain both
459 pathogen defense and morphological differences between ecotypes, but show a limited
460 effectiveness in the south. This pattern raises important questions about the drivers of genetic
461 architecture of pathogen resistance and underscores the importance of assaying pathogen
462 resistance across both time and space to capture the inherent variability in the interplay of biotic
463 and abiotic drivers of genetic change. These loci may allow for more effective breeding
464 strategies for rust resistance, if there are not trade-offs with other traits, such as cold tolerance.
465 The role of rust in differentiating these ecotypes illustrates the synergistic role pathogens play in
466 the evolution of different ecotypes and ultimately contributing to genetic variation within
467 species.

468

469

470

471

472

473

474

475

476

477

478

479

480

481

482

483

484 **References**

485 Agrios GN. 1997. Control of plant diseases. *Plant Pathol.* 5:295–357

486 Alfano JR, Collmer A. 2004. Type III secretion system effector proteins: double agents in bacterial disease and plant
487 defense. *Annu. Rev. Phytopathol.* 42:385–414

- 488 Ali S, Gladieux P, Leconte M, Gautier A, Justesen AF, et al. 2014. Origin, migration routes and worldwide
489 population genetic structure of the wheat yellow rust pathogen *Puccinia striiformis* f. sp. *tritici*. *PLoS*
490 *Pathog.* 10(1):e1003903
- 491 Arnold AE, Herre EA. 2003. Canopy cover and leaf age affect colonization by tropical fungal endophytes:
492 ecological pattern and process in *Theobroma cacao* (Malvaceae). *Mycologia.* 95(3):388–98
- 493 Arnold AE, Lutzoni F. 2007. Diversity and host range of foliar fungal endophytes: are tropical leaves biodiversity
494 hotspots? *Ecology.* 88(3):541–49
- 495 Beavis WD. 1998. QTL analyses: power, precision, and accuracy. *Mol. dissection complex Trait.* 1998:145–62
- 496 Broman KW, Sen S. 2009. *A Guide to QTL Mapping with R/qtl*, Vol. 46. Springer
- 497 Broman KW, Wu H, Sen S, Churchill GA. 2003. R/qtl: QTL mapping in experimental crosses. *Bioinformatics.*
498 19(7):889–90
- 499 Bueker B, Eberlein C, Gladieux P, Schaefer A, Snirc A, et al. 2016. Distribution and population structure of the
500 anther smut *Microbotryum silenes-acaulis* parasitizing an arctic–alpine plant. *Mol. Ecol.* 25(3):811–24
- 501 Casler MD, Vogel KP, Taliaferro CM, Wynia RL. 2004. Latitudinal adaptation of switchgrass populations. *Crop*
502 *Sci.* 44(1):293–303
- 503 Casler MD. 2012. Switchgrass breeding, genetics, and genomics. In *Switchgrass*, pp. 29–53. Springer
- 504 Casler MD, Vogel KP, Taliaferro CM, Ehlke NJ, Berdahl JD, et al. 2007. Latitudinal and longitudinal adaptation of
505 switchgrass populations. *Crop Sci.* 47(6):2249–60
- 506 Clausen J, Keck DD, Hiesey WM. 1940. Experimental studies on the nature of species. I. Effect of varied
507 environments on western North American plants. *Exp. Stud. Nat. species. I. Eff. varied Environ. West.*
508 *North Am. plants.*
- 509 Cornelius DR, Johnston CO. 1941. Differences in plant type and reaction to rust among several collections of
510 *Panicum virgatum* L. *J. Am. Soc. Agron.*
- 511 Corwin JA, Kliebenstein DJ. 2017. Quantitative resistance: more than just perception of a pathogen. *Plant Cell.*
512 29(4):655–65
- 513 Crémieux L, Bischoff A, Šmilauerová M, Lawson CS, Mortimer SR, et al. 2008. Potential contribution of natural
514 enemies to patterns of local adaptation in plants. *New Phytol.* 180(2):524–33
- 515 Demers JE, Liu M, Hambleton S, Castlebury LA. 2017. Rust fungi on *Panicum*. *Mycologia.* 109(1):1–17
- 516 Dodds PN, Lawrence GJ, Catanzariti A-M, Teh T, Wang C-I, et al. 2006. Direct protein interaction underlies gene-
517 for-gene specificity and coevolution of the flax resistance genes and flax rust avirulence genes. *Proc. Natl.*
518 *Acad. Sci.* 103(23):8888–93
- 519 Doke N. 1983. Involvement of superoxide anion generation in the hypersensitive response of potato tuber tissues to
520 infection with an incompatible race of *Phytophthora infestans* and to the hyphal wall components. *Physiol.*
521 *Plant Pathol.* 23(3):345–57
- 522 Eversmeyer MG, Kramer CL. 2000. Epidemiology of wheat leaf and stem rust in the central great plains of the
523 USA. *Annu. Rev. Phytopathol.* 38(1):491–513

- 524 Fournier-Level A, Korte A, Cooper MD, Nordborg M, Schmitt J, Wilczek AM. 2011. A map of local adaptation in
525 *Arabidopsis thaliana*. *Science* (80-.). 334(6052):86–89
- 526 Franklin KA, Wigge PA. 2014. *Temperature and plant development*. Wiley Online Library
- 527 Fu D, Uauy C, Distelfeld A, Blechl A, Epstein L, et al. 2009. A kinase-START gene confers temperature-dependent
528 resistance to wheat stripe rust. *Science* (80-.). 323(5919):1357–60
- 529 Gagneux S, DeRiemer K, Van T, Kato-Maeda M, De Jong BC, et al. 2006. Variable host–pathogen compatibility in
530 *Mycobacterium tuberculosis*. *Proc. Natl. Acad. Sci.* 103(8):2869–73
- 531 German SE, Kolmer JA. 1992. Effect of gene Lr34 in the enhancement of resistance to leaf rust of wheat. *Theor.*
532 *Appl. Genet.* 84(1–2):97–105
- 533 Giraud T, Koskella B, Laine A. 2017. Introduction: microbial local adaptation: insights from natural populations,
534 genomics and experimental evolution. *Mol. Ecol.* 26(7):1703–10
- 535 Gleason HA, Cronquist A. 1991. *Manual of vascular plants of northeastern United States and adjacent Canada*,
536 Vol. 834. New York Botanical Garden Bronx, NY
- 537 Grøndahl E, Ehlers BK. 2008. Local adaptation to biotic factors: reciprocal transplants of four species associated
538 with aromatic *Thymus pulegioides* and *T. serpyllum*. *J. Ecol.* 96(5):981–92
- 539 He L, Wu W, Zinta G, Yang L, Wang D, et al. 2018. A naturally occurring epiallele associates with leaf senescence
540 and local climate adaptation in *Arabidopsis* accessions. *Nat. Commun.* 9(1):460
- 541 Herms DA, Mattson WJ. 1992. The dilemma of plants: to grow or defend. *Q. Rev. Biol.* 67(3):283–335
- 542 Hooper L V, Gordon JI. 2001. Commensal host-bacterial relationships in the gut. *Science* (80-.). 292(5519):1115–
543 18
- 544 Jeger MJ, Viljanen-Rollinson SLH. 2001. The use of the area under the disease-progress curve (AUDPC) to assess
545 quantitative disease resistance in crop cultivars. *Theor. Appl. Genet.* 102(1):32–40
- 546 Jones JDG, Dangl JL. 2006. The plant immune system. *Nature.* 444(7117):323
- 547 Kawecki TJ, Ebert D. 2004. Conceptual issues in local adaptation. *Ecol. Lett.* 7(12):1225–41
- 548 Kenaley SC, Quan M, Aime MC, Bergstrom GC. 2018. New insight into the species diversity and life cycles of rust
549 fungi (Pucciniales) affecting bioenergy switchgrass (*Panicum virgatum*) in the Eastern and Central United
550 States. *Mycol. Prog.* 17(11):1251–67
- 551 Kliebenstein DJ. 2016. False idolatry of the mythical growth versus immunity tradeoff in molecular systems plant
552 pathology. *Physiol. Mol. Plant Pathol.* 95:55–59
- 553 Kniskern JM, Rausher MD. 2006. Major-gene resistance to the rust pathogen *Coleosporium ipomoeae* is common in
554 natural populations of *Ipomoea purpurea*. *New Phytol.* 171(1):137–44
- 555 Kolmer JA. 2005. Tracking wheat rust on a continental scale. *Curr. Opin. Plant Biol.* 8(4):441–49
- 556 Kwak I-Y, Moore CR, Spalding EP, Broman KW. 2014. A simple regression-based method to map quantitative trait
557 loci underlying function-valued phenotypes. *Genetics.* 197(4):1409–16
- 558 Kwak I-Y, Moore CR, Spalding EP, Broman KW. 2016. Mapping quantitative trait loci underlying function-valued
559 traits using functional principal component analysis and multi-trait mapping. *G3 Genes, Genomes, Genet.*
560 6(1):79–86

- 561 Lee DK, Parrish AS, Voigt TB. 2014. Switchgrass and giant *Miscanthus* agronomy. In *Engineering and science of*
562 *biomass feedstock production and provision*, pp. 37–59. Springer
- 563 Leimu R, Fischer M. 2008. A meta-analysis of local adaptation in plants. *PLoS One*. 3(12):e4010
- 564 Lesaffre E, Lawson AB. 2012. *Bayesian biostatistics*. John Wiley & Sons
- 565 Lovell JT, Shakirov E V, Schwartz S, Lowry DB, Aspinwall MJ, et al. 2016. Promises and challenges of eco-
566 physiological genomics in the field: tests of drought responses in switchgrass. *Plant Physiol*. 172(2):734–
567 48
- 568 Lowry DB, Behrman KD, Grabowski P, Morris GP, Kiniry JR, Juenger TE. 2014. Adaptations between ecotypes
569 and along environmental gradients in *Panicum virgatum*. *Am. Nat.* 183(5):682–92
- 570 Lowry DB, Willis JH. 2010. A widespread chromosomal inversion polymorphism contributes to a major life-history
571 transition, local adaptation, and reproductive isolation. *PLoS Biol*. 8(9):e1000500
- 572 Macel M, Lawson CS, Mortimer SR, Šmilauerova M, Bischoff A, et al. 2007. Climate vs. soil factors in local
573 adaptation of two common plant species. *Ecology*. 88(2):424–33
- 574 Magarey RD, Sutton TB, Thayer CL. 2005. A simple generic infection model for foliar fungal plant pathogens.
575 *Phytopathology*. 95(1):92–100
- 576 McDonald BA, Linde C. 2002. Pathogen population genetics, evolutionary potential, and durable resistance. *Annu.*
577 *Rev. Phytopathol*. 40(1):349–79
- 578 Mckay JK, Richards JH, Mitchell-Olds T. 2003. Genetics of drought adaptation in *Arabidopsis thaliana*: I.
579 Pleiotropy contributes to genetic correlations among ecological traits. *Mol. Ecol*. 12(5):1137–51
- 580 McNeal FH, Konzak CF, Smith EP, Tate WS, Russell TS. 1971. *A uniform system for recording and processing*
581 *cereal research data*. USDA-ARS.
- 582 Michelmore RW, Christopoulou M, Caldwell KS. 2013. Impacts of resistance gene genetics, function, and evolution
583 on a durable future. *Annu. Rev. Phytopathol*. 51:291–319
- 584 Milano ER, Lowry DB, Juenger TE. 2016. The genetic basis of upland/lowland ecotype divergence in switchgrass
585 (*Panicum virgatum*). *G3 Genes, Genomes, Genet*. 6(11):3561–70
- 586 Moran NA, McCutcheon JP, Nakabachi A. 2008. Genomics and evolution of heritable bacterial symbionts. *Annu.*
587 *Rev. Genet*. 42:165–90
- 588 Morris GP, Grabowski PP, Borevitz JO. 2011. Genomic diversity in switchgrass (*Panicum virgatum*): from the
589 continental scale to a dune landscape. *Mol. Ecol*. 20(23):4938–52
- 590 Mundt CC. 2014. Durable resistance: a key to sustainable management of pathogens and pests. *Infect. Genet. Evol.*
591 27:446–55
- 592 Mursinoff S, Tack AJM. 2017. Spatial variation in soil biota mediates plant adaptation to a foliar pathogen. *New*
593 *Phytol*. 214(2):644–54
- 594 Parrish DJ, Casler MD, Monti A. 2012. The evolution of switchgrass as an energy crop. In *Switchgrass*, pp. 1–28.
595 Springer
- 596 Peixoto M de M, Sage RF. 2016. Improved experimental protocols to evaluate cold tolerance thresholds in
597 *Miscanthus* and switchgrass rhizomes. *Gcb Bioenergy*. 8(2):257–68

- 598 Penczykowski RM, Laine A, Koskella B. 2016. Understanding the ecology and evolution of host–parasite
599 interactions across scales. *Evol. Appl.* 9(1):37–52
- 600 Perchepped L, Dogimont C, Pitrat M. 2005. Strain-specific and recessive QTLs involved in the control of partial
601 resistance to *Fusarium oxysporum f. sp. melonis* race 1.2 in a recombinant inbred line population of melon.
602 *Theor. Appl. Genet.* 111(1):65–74
- 603 Price N, Moyers BT, Lopez L, Lasky JR, Monroe JG, et al. 2018. Combining population genomics and fitness QTLs
604 to identify the genetics of local adaptation in *Arabidopsis thaliana*. *Proc. Natl. Acad. Sci.* 115(19):5028–33
- 605 Price N, Moyers BT, Lopez L, Lasky JR, Monroe JG, et al. 2018. Combining population genomics and fitness QTLs
606 to identify the genetics of local adaptation in *Arabidopsis thaliana*. *Proc. Natl. Acad. Sci.* 115(19):5028–33
- 607 Roelfs AP. 1992. *Rust diseases of wheat: concepts and methods of disease management*. Cimmyt
- 608 Simms EL, Triplett J. 1994. Costs and Benefits of Plant Responses to Disease : Resistance and Tolerance. *Evolution*
609 (*N. Y.*) 48(6):1973–85
- 610 Sykes VR, Allen FL, Mielenz JR, Stewart CN, Windham MT, et al. 2016. Reduction of ethanol yield from
611 switchgrass infected with rust caused by *Puccinia emaculata*. *BioEnergy Res.* 9(1):239–47
- 612 Tian D, Traw MB, Chen JQ, Kreitman M, Bergelson J. 2003. Fitness costs of R-gene-mediated resistance in
613 *Arabidopsis thaliana*. *Nature.* 423(6935):74
- 614 Traw MB, Kniskern JM, Bergelson J. 2007. SAR increases fitness of *Arabidopsis thaliana* in the presence of natural
615 bacterial pathogens. *Evol. Int. J. Org. Evol.* 61(10):2444–49
- 616 Uppalapati SR, Serba DD, Ishiga Y, Szabo LJ, Mittal S, et al. 2013. Characterization of the rust fungus, *Puccinia*
617 *emaculata*, and evaluation of genetic variability for rust resistance in switchgrass populations. *Bioenergy*
618 *Res.* 6(2):458–68
- 619 Van Leur JAG, Ceccarelli S, Grando S. 1989. Diversity for disease resistance in barley landraces from Syria and
620 Jordan. *Plant Breed.* 103(4):324–35
- 621 Wadl PA, Dean D, Li Y, Vito LM, Scheffler BE, et al. 2011. Development and characterization of microsatellites
622 for switchgrass rust fungus (*Puccinia emaculata*). *Conserv. Genet. Resour.* 3(1):185–88
- 623 Weller DM, Raaijmakers JM, Gardener BBM, Thomashow LS. 2002. Microbial populations responsible for specific
624 soil suppressiveness to plant pathogens. *Annu. Rev. Phytopathol.* 40(1):309–48
- 625 Wickham H, Wickham MH. 2007. The ggplot package
- 626 Woolhouse MEJ, Webster JP, Domingo E, Charlesworth B, Levin BR. 2002. Biological and biomedical
627 implications of the co-evolution of pathogens and their hosts. *Nat. Genet.* 32(4):569
- 628 Xu S. 2003. Theoretical basis of the Beavis effect. *Genetics.* 165(4):2259–68
- 629 Zhang Y, Zalapa JE, Jakubowski AR, Price DL, Acharya A, et al. 2011. Post-glacial evolution of *Panicum*
630 *virgatum*: centers of diversity and gene pools revealed by SSR markers and cpDNA sequences. *Genetica.*
631 139(7):933
- 632 Zhu Y, Qian W, Hua J. 2010. Temperature modulates plant defense responses through NB-LRR proteins. *PLoS*
633 *Pathog.* 6(4):e1000844
- 634